Journal of University of Science and Technology Beijing
Volume 14, Number 1, February 2007, Page 77

Materials

Adsorption behavior of heavy metal ions by carbon nanotubes grown on microsized Al_2O_3 particles

Shu-Huei Hsieh[1] *and Jao-Jia Horng*[2]

1) Department of Materials Science and Engineering, Formosa University, Yunlin, China Taipei

2) Department of Safety, Health and Environmental Engineering, Yunlin University of Science and Technology, Yunlin, China Taipei

(Received 2006-03-05)

Abstract: Carbon nanotubes (CNTs) were grown on the surface of microsized Al_2O_3 particles in CH_4 atmosphere at 700°C under the catalysis of Fe-Ni nanoparticles. The CNTs on Al_2O_3 were used for adsorbing Pb^{2+}, Cu^{2+}, and Cd^{2+} from the solution and the results were compared with active carbon powders, commercial carbon nanotubes, and Al_2O_3 particles. The as-grown CNTs/Al_2O_3 have demonstrated extraordinary absorption capacity with further treatment or oxidation, as well as hydrophilic ability that other CNTs lacked. The adsorption capacity of CNTs on Al_2O_3 is superior to other adsorbents and the preference order of adsorption on composite Al_2O_3 is Pb^{2+}>Cu^{2+}>Cd^{2+}. It seemed that the adsorption of those Pb^{2+}, Cu^{2+}, and Cd^{2+} did not change the surface properties of composite particles. The adsorption behaviors of Pb^{2+}, Cu^{2+}, and Cd^{2+} by CNTs on Al_2O_3 match well with the Langmuir isothermal adsorption model and the second order kinetic model. The calculated saturation amount adsorbed by 1 g of CNTs on Al_2O_3 are 67.11, 26.59, and 8.89 mg/g for Pb^{2+}, Cu^{2+}, and Cd^{2+} in single adsorption test, respectively.

Key words: carbon nanotube; heavy metal; adsorption; alumina

1. Introduction

Heavy metal ions such as Pb^{2+}, Cd^{2+}, Cu^{2+}, Ni^{2+}, Cr^{6+} and so on, are toxic to plants, animals, and human beings because of their cumulative and interfering effects on bio-chemical functions while entering cells via various pathways. Water contaminated by heavy metal ions had become much more serious with a rapid development of industries and competitive use of fresh water in many parts of world. Therefore, the removal of heavy metal ions from water has become an important subject today.

Many techniques and methods to remove heavy metal ions from water have been developed, such as ion-exchange, evaporation and concentration, chemical precipitation, reverse osmosis, adsorption, and electrolysis [1]. Considering from the economy and efficiency point of view, adsorption is regarded as the most promising and widely used method among all these. Numerous materials can be used as adsorbents to remove heavy metal ions from water, such as metal oxide [2], active carbon [3], sepiolite [4], chitin [5], biosorbent [6], metal sulfide [7], resin [8], and so on. The search for new and more effective materials to be used as adsorbents is a continuous effort for many researchers.

As carbon nanotubes (CNTs) were discovered by Iijima in 1991 [9], they have been widely studied for their excellent properties and applications. Besides applying to planar display [10], fuel cells [11], secondary batteries [12], and electronics [13-14], CNTs are applied to environmental protection as absorbents for heavy metal ions and anions in solutions [1, 15-19]. Their adsorption capacity for fluoride is 15-25 times higher than an active carbon [16]. Because CNTs possess a high chemical and thermal stability and a large specific surface area, they have been applied to remove heavy metal ions from aqueous solution [1, 15, 17-21]. The results of these studies show that CNT is a promising candidate for adsorption of heavy metal ions. The adsorption capacity of CNTs is greatly dependent on their properties such as microstructure, crystallinity, surface state, and so on. These properties of CNTs are determined by different factors in the manufacturing process, such as growth method, growth conditions, and treatment after growth [1, 19-20].

In the previous studies [20-21], CNTs were grown on the surface of microsized Al_2O_3 particles by the chemical vapor deposition (CVD) technique and used to adsorb Pb^{2+}, Cd^{2+}, and Cu^{2+} from water. The adsorption capacity of CNTs was also compared with active carbon powders, commercial CNTs and Al_2O_3 particles.

Corresponding author: Jao-Jia Horng, **E-mail:** horngjj@hotmail.com

In addition, the preference and competitiveness of metal ions were also studied to understand the possible kinetic and adsorption models.

2. Experimental materials and methods

In this study, CNTs were grown on the surface of micro-sized α-Al_2O_3 particles. Before growth of CNTs, Fe-Ni nanoparticles were deposited on the surface of Al_2O_3 particles as catalysts by the electroless plating method. The growth of CNTs on Al_2O_3 (denoted by CNTs/Al_2O_3 hereafter) was performed in CH_4 atmosphere at 700°C [20-21]. The as-grown CNTs/Al_2O_3 (without further treatment or oxidation) was used as adsorbent for adsorption of Pb^{2+}, Cu^{2+}, and Cd^{2+} from water. The adsorption capacity of composite CNTs/Al_2O_3 and those of active carbon powders (Merk), commercial multi-wall CNTs (Conyuan MWCNTs 2040), and α-Al_2O_3 particles were compared and analyzed, and the composite CNTs/Al_2O_3 were used to adsorb heavy metal ions from aqueous solutions.

Before adsorption test, adsorbents were characterized by various methods. The specific area was determined using the BET (Brunauer-Emmett-Teller) method (Micrometrics ASAP-2010). The surface morphology was observed using a field emission scanning electron microscope (FESEM) (JEOL JSM-6700 F) operated at 20 kV. The microstructure and crystallinity were investigated using a transmission electron microscope (TEM) (JEOL JEM-2010) operated at 200 kV. The phases were analyzed using an X-ray diffraction meter (XRD) (Siemens, D5000).

Several adsorption tests were performed in this study: for single/dual and three metal ion adsorption, for equilibrium adsorption, for the effect of different solution pHs, and for the effect of adsorbent amount on the adsorption.

For the test of single metal ion adsorption, Pb^{2+} solution with a concentration of 5-40 mg/L, Cu^{2+} solution with a concentration of 2-25 mg/L, and Cd^{2+} solution with a concentration of 2-15 mg/L were prepared from nitrate salts respectively. In each single metal ion adsorption test, 0.05 g of adsorbent was used for 100 mL of ion solution. The ion solution with adsorbent was vibrated on a rotary vibrator (TS-580 batch shaker) for 4 h [20].

For the test of equilibrium adsorption, Pb^{2+}, Cu^{2+}, and Cd^{2+} solutions of 40 mg/L were prepared from nitrate respectively. The pH values of all solutions were adjusted to 5 by 0.1 mol/L HNO_3 and 0.1 mol/L NaOH. An adsorbent of 0.1 g was put into 200 mL of ion solution. The vibration time for various samples is 30, 60, 120, 180, 240, 300, and 360 min, respectively.

For the test of the effect of pH value on adsorption, Pb^{2+}, Cu^{2+}, and Cd^{2+} solutions of 40 mg/L were prepared from nitrate respectively. The pH values of various solutions were adjusted from 2 to 11 respectively. An adsorbent of 0.1 g was added to each solution of 100 mL. Each solution with the adsorbent was vibrated for 4 h.

For the test of the adsorbent amount's effect on adsorption, Pb^{2+}, Cu^{2+}, and Cd^{2+} solutions of 40 mg/L were prepared from nitrate. An adsorbent of 0.05, 0.1, 0.15, 0.2, 0.25, and 0.3 g was added to various solutions of 100 mL respectively. Vibration time for all solutions is 4 h.

For all tests, the concentrations of metal ions in the solution were measured before and after adsorption using an inductively coupled plasma atomic emission spectrometer (ICP-AES) (GBC Integra XMP) and the adsorbed amount of heavy metal was calculated from the concentration of these metal ions.

3. Results and discussion

The FESEM image of CNTs/Al_2O_3 is shown in Fig. 1. It is clear that the as-grown CNTs on Al_2O_3 are curved and tangled with each other and about 30-80 nm in diameter and several micrometers in length. The TEM image of CNTs on Al_2O_3 is shown in Fig. 2, where multi-walled CNTs with Fe-Ni nanoparticles were identified using TEM/EDS on the tips of CNT. The mass ratio for CNTs, Fe-Ni nanoparticles, and Al_2O_3 was determined to be at 32wt%, 12wt%, and 56wt%, respectively [20].

The XRD diagram in Fig. 3 shows that there are α-Al_2O_3, CNTs, and FeNi phases in the composite CNTs/Al_2O_3. The specific areas of Al_2O_3 particles, active carbon powders, commercial CNTs, and CNTs/Al_2O_3 are determined to be 9.13, 815.69, 95.68, and 18.61 m^2/g, respectively [20]. And, the specific area of CNTs alone increases to 66.85 m^2/g from 18.61 m^2/g of composite CNTs/Al_2O_3. This area is rather small when compared to 95.68 m^2/g of commercial CNTs and 815.69 m^2/g of activated carbon.

The results of equilibrium adsorption tests are shown in Figs. 4(a)-(d) for Al_2O_3 particles, active carbon powders, commercial CNTs, and CNTs/Al_2O_3, respectively. In Fig. 4, the abscissa denotes time (in minutes) of adsorption and the ordinate (q_e) denotes the metal weight (in mg) adsorbed by 1 g of adsorbent in the given adsorption periods. These results show that almost all the adsorbed metal amounts have nearly

reached the maximum adsorption in 240 min (4 h). The preference and capacity order of adsorbed $Pb^{2+}>Cu^{2+}>Cd^{2+}$ is similar for adsorbents of Al_2O_3 particles, active carbon powders, commercial CNTs, and CNTs/Al_2O_3. The relative order of adsorption capacity is CNTs/Al_2O_3>active carbon powders>commercial CNTs>Al_2O_3 for Pb and Cu, but CNTs/Al_2O_3>commercial CNTs>active carbon powders>Al_2O_3 for Cd. For adsorbent of CNTs/Al_2O_3, the maximum adsorbed amounts for Pb, Cu, and Cd are 36, 22, and 8.4 mg/g which are the largest among those adsorbents.

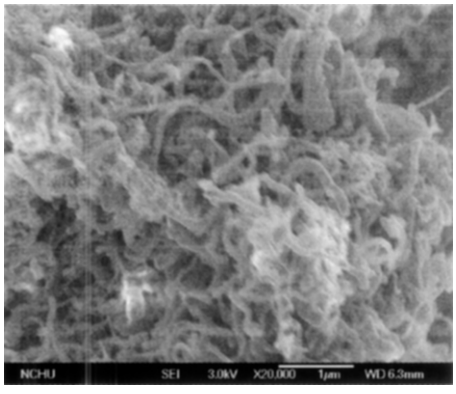

Fig. 1. FE-SEM morphology of CNTs on aluminium oxide (CNTs/Al_2O_3).

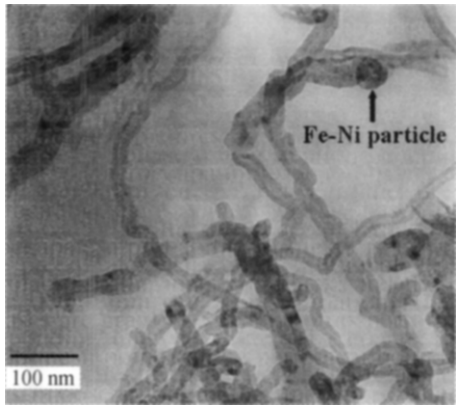

Fig. 2. TEM morphology of CNTs on aluminium oxide (CNTs/Al_2O_3).

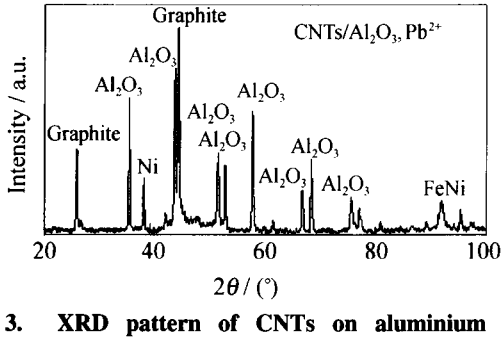

Fig. 3. XRD pattern of CNTs on aluminium oxide (CNTs/Al_2O_3).

Figs. 5(a)-(d) show the adsorption isotherms of single metal ions adsorption. In Fig. 5, the abscissa C_e (in mg/L) is the equilibrium concentration of metal ion in a solution and the ordinate q_e (in mg/g) is the metal amount adsorbed by 1 g of adsorbent after an adsorption time of 4 h. These results show that the order of q_e is $Pb^{2+}>Cu^{2+}>Cd^{2+}$ at all C_e for all adsorbents and the q_e of CNTs/Al_2O_3 at all C_e is the largest among the four adsorbents. On comparing the adsorption capacity of Pb^{2+}, Cu^{2+}, and Cd^{2+}, CNTs/Al_2O_3 is found to be superior to commercial CNTs without further treatment [20]. Other researchers have also achieved similar or better adsorption capacity but they all have required further treatment or oxidation of CNTs [1,18-19].

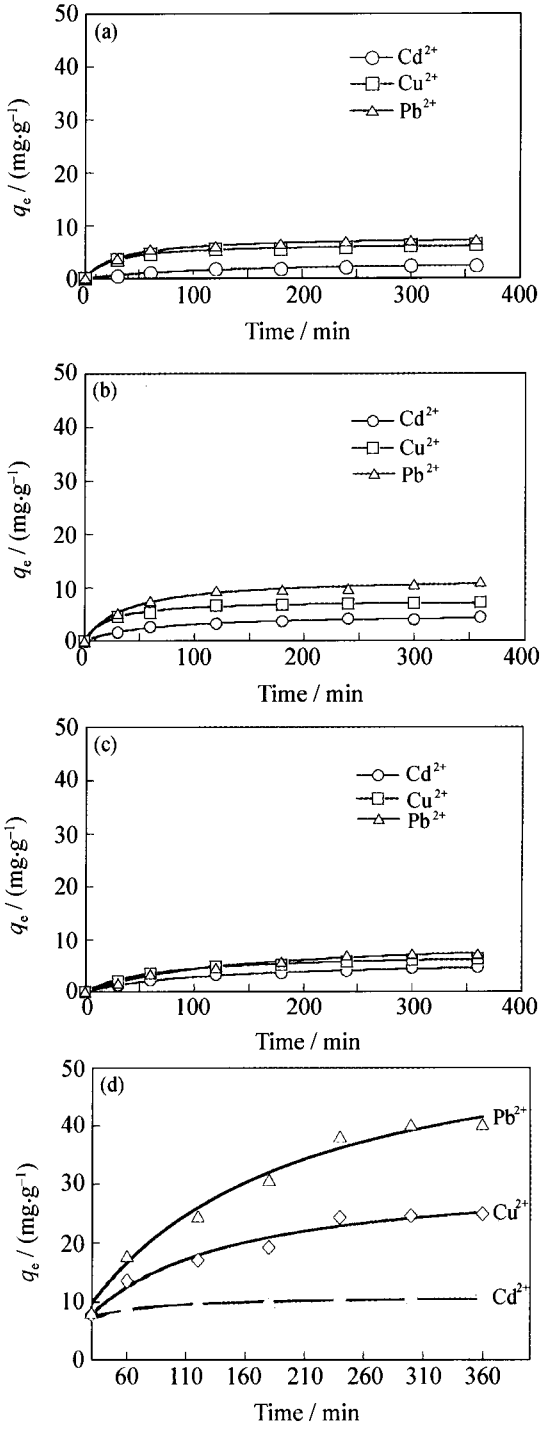

Fig. 4. Equilibrium adsorptions of Pb^{+2}, Cu^{+2}, and Cd^{+2} adsorbed by Al_2O_3 particles (a), active carbon powders (b), commercial CNTs (c), and CNTs/Al_2O_3 (d).

To further understand this phenomenon, a sedimentation test for CNTs/Al_2O_3 and commercial CNTs in deionized water was performed. After 2 min of sedimentation, commercial CNTs quickly settled down and CNTs/Al_2O_3 remained mixed in solution as shown in Fig. 6. This phenomenon implied that the commercial CNTs were easy to agglomerate and settle so that they have a lesser opportunity to adsorb metal ions in solutions, compared to the CNTs/Al_2O_3. Other researchers did not present their CNTs with similar dispersion property in water solution as this study had demonstrated.

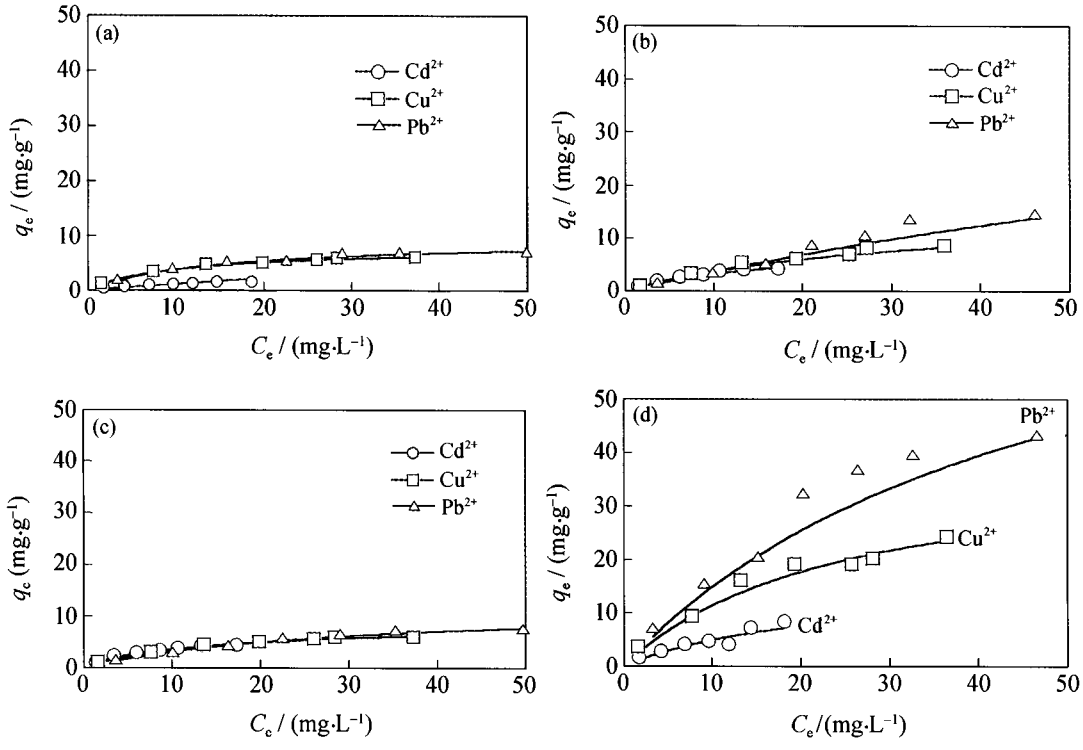

Fig. 5. Single metal ion adsorptions of Pb^{2+}, Cu^{2+}, and Cd^{2+} adsorbed by Al_2O_3 particles (a), active carbon powders (b), commercial CNTs (c), and CNTs/Al_2O_3 (d).

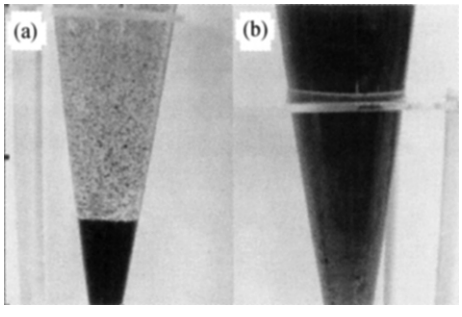

Fig. 6. Images of settlement in water of commercial CNTs (a) and CNTs/Al_2O_3 (b) after 2 min.

The adsorption of Pb^{+2}, Cu^{+2}, and Cd^{+2} from water by CNTs/Al_2O_3, commercial CNTs, active carbon powders, and Al_2O_3 particles can be assumed to have a behavior fitting with the isothermal adsorption model that is the adsorbate keeps a dynamic equilibrium between the adsorption and desorption at a fixed temperature. For the isothermal adsorption model, there are some adsorption isotherms as follows.

Langmuir isotherm:

$$\frac{1}{q_e}=\frac{1}{q_m}+\frac{1}{q_m K_e C_e},$$

Freundlich isotherm:

$$q_e = K_f C_e^{\frac{1}{n}},$$

And BET isotherm:

$$q_e = \beta C_e q_m / \left\{(C_s - C_e)\left[1+(\beta-1)\left(\frac{C_e}{C_s}\right)\right]\right\},$$

where q_e (in mg/g) is the adsorbate amount adsorbed by 1 g of absorbent, C_e (in mg/g) is the equilibrium concentration of adsorbate in the solution, q_m (in mg/g) is the saturation amount of the adsorbate adsorbed by one gram of absorbent, and K_e, K_f, n, β, and C_s are constants. The results of single metal ion adsorptions of Pb^{2+}, Cu^{2+}, and Cd^{2+} adsorbed by Al_2O_3 particles, active carbon powders, commercial CNTs and CNT/Al_2O_3, as shown in Figs. 5(a)-(d) were tried to fit these adsorption isotherms and their results were shown in Tables 1 and 2. From the values of coefficient of determination (R^2), the Langmuir isotherm is the best model for all absorbents in this study. This means that the adsorbates containing Pb^{2+}, Cu^{2+}, and Cd^{2+} were adsorbed in such a manner that only one atomic layer of adsorbate can be adsorbed and distributed uniformly on the surface of

the adsorbents. According to the Langmuir adsorption model, the saturation amounts, q_m, of Pb^{2+}, Cu^{2+}, and Cd^{2+} adsorbed by 1 g of CNTs/Al_2O_3 are 67.11, 26.59 and 8.89 mg/g respectively, which are much larger than that of the commercial CNTs and similar in some cases [1,18-19]. However, those studies used the CNTs that required further treatment or oxidation.

Table 1. Isothermal adsorption models for adsorption of Pb^{2+}, Cu^{2+}, and Cd^{2+} by various adsorbents

Adsorbent	Metal ion	Langmuir			Freundlich			pH range
		q_m / (mg·g^{-1})	K_e / (L·mg^{-1})	R^2	n	K_f / (L·mg^{-1})	R^2	
α-Al_2O_3	Pb^{2+}	8.92	0.09	0.997	2.12	1.30	0.953	5.87-6.01
	Cu^{2+}	6.97	0.16	0.997	2.08	1.22	0.971	5.80-6.29
	Cd^{2+}	2.00	0.16	0.994	1.84	0.34	0.984	6.30-6.53
PAC[1]	Pb^{2+}	33.78	0.01	0.983	1.09	0.49	0.977	5.85-6.02
	Cu^{2+}	11.79	0.06	0.998	1.48	0.86	0.988	5.97-6.17
	Cd^{2+}	5.89	0.17	0.996	1.76	0.98	0.987	6.63-6.86
CNT[2]	Pb^{2+}	11.23	0.04	0.993	1.52	0.68	0.979	5.08-5.14
	Cu^{2+}	7.14	0.12	0.996	1.86	0.99	0.980	4.82-5.11
	Cd^{2+}	6.19	0.18	0.997	1.94	1.94	0.964	5.12-5.19
CNT/ Al_2O_3	Pb^{2+}	67.11	0.04	0.989	1.39	3.22	0.974	5.05-5.34
	Cu^{2+}	26.59	0.10	0.987	1.66	2.91	0.980	5.25-5.52
	Cd^{2+}	8.89	0.13	0.956	1.55	1.17	0.926	5.28-5.78

Note: 1 represents active carbon powders, 2 represents commercial CNTs.

Table 2. Multilayer adsorption model for adsorption of Pb^{+2}, Cu^{+2}, and Cd^{+2} by various adsorbents

Adsorbent	Metal ion	BET			
		q_m / (mg·g^{-1})	β/ (L·mg^{-1})	R^2	Equation
α-Al_2O_3	Pb^{2+}	8.63×10^{-3}	–0.29	0.865	$Y = 513.61x–398.09$
	Cu^{2+}	0.01	–0.40	0.823	$Y = 279.73x–199.86$
	Cd^{2+}	0.02	–0.11	0.861	$Y = 443.24x–398.68$
PAC[1]	Pb^{2+}	6.28×10^{-3}	–0.29	0.204	$Y = 709.61x–550.34$
	Cu^{2+}	9.43×10^{-3}	–0.32	0.819	$Y = 433.36x–327.42$
	Cd^{2+}	0.02	–0.39	0.887	$Y = 178.46x–128.26$
CNT[2]	Pb^{2+}	6.49×10^{-3}	–0.20	0.892	$Y = 924.77x–770.83$
	Cu^{2+}	0.01	–0.33	0.830	$Y = 340.74x–255.24$
	Cd^{2+}	0.02	–0.43	0.917	$Y = 154.32x–107.69$
CNT/Al_2O_3	Pb^{2+}	1.86×10^{-3}	–0.36	0.848	$Y = 2016.2x–1497.2$
	Cu^{2+}	3.47×10^{-3}	–0.36	0.879	$Y = 1078x–790.14$
	Cd^{2+}	5.58×10^{-3}	–0.15	0.741	$Y = 1337.3x–1158$

Note: 1 represents active carbon powders, 2 represents commercial CNTs.

Furthermore, the specific areas of CNTs/Al_2O_3 before and after adsorption were also measured by BET method and the results were shown in Table 3. The saturation amounts q_m of Pb^{2+}, Cu^{2+}, and Cd^{2+} adsorbed by CNTs/Al_2O_3 were also listed in Table 4. The ratio of the reduced specific area of CNTs/Al_2O_3 after adsorption to that of CNTs/Al_2O_3 before adsorption for Pb^{2+}, Cu^{2+}, and Cd^{2+} is 19%, 10% and 7.8%, respectively. In addition, the adsorption of Pb^{2+}, Cu^{2+}, and Cd^{2+} only occupied a small surface area of CNTs/Al_2O_3. The reduced specific area is the difference between the specific area before and after adsorption. The fourth column of Table 3 shows the amounts of heavy metals adsorbed by one unit of area of CNTs/Al_2O_3, which are obtained by calculation, that is, dividing the saturation amount by the reduced specific area. It also demonstrates that the order of metal amount adsorbed by CNTs/Al_2O_3 is Pb^{2+}>Cu^{2+}>Cd^{2+}. As for the kinetic behavior of adsorption in liquids, there in general are two models. The first order kinetic model can be expressed by $\frac{dq_t}{dt} = k_1(q_e - q_t)$, where k_1 is the first order rate constant, in min^{-1}; q_e and q_t, in mg/g, are the metal amounts adsorbed by adsorbent at time $t = \infty$ and t respectively. The equation becomes $\lg(q_e - q_t) = \lg q_e - \frac{k_1}{2.303}t$ after integration. The second order kinetic model is expressed by

$\frac{dq_t}{dt} = k_2(q_e - q_t)^2$, where k_2 is the second order rate constant, in $L \cdot mg^{-1} \cdot min^{-1}$, and it becomes $\frac{t}{q_t} = \frac{1}{k_2 q_e^2} + \frac{1}{q_e} t$ after integration. The data in Figs. 4(a)-(d) can be put in the first and second order kinetic model respectively and the diagrams of $\lg(q_e - q_t)$ *vs* t and t/q_t *vs* t are made. From the slope and interception distance of the regress line, the k_1, k_2, and q_e in the equations can be obtained, which are listed in Table 4. From the coefficient of determination (R^2) and the comparisons between $q_{m,exp}$, the experimental value of saturation amount, and $q_{m,cal}$, the calculated value of saturation amount which is equal to q_e in the equations, the kinetic behavior of the adsorption in this study matches well with the second order kinetic model.

Table 3. Specific surface area of $CNTs/Al_2O_3$ before and after adsorption of Pb^{2+}, Cu^{2+}, and Cd^{2+}

Adsorbent material	Specific surface area (E) / $(m^2 \cdot g^{-1})$	Saturation amounts q_m (F) / $(mg \cdot g^{-1})$	Adsorbed mass of metal ion per unit specific area (G) / $(mg \cdot m^{-2})$
($CNTs/Al_2O_3$) (a)	18.61	—	—
($CNTs/Al_2O_3$) after adsorption of Pb^{2+} (b)	15.06	67.11	20.03
($CNTs/Al_2O_3$) after adsorption of Cu^{2+} (b)	16.69	26.59	13.85
($CNTs/Al_2O_3$) after adsorption of Cd^{2+} (b)	17.15	8.89	6.09

Note: E represents the data measured by gas adsorption, q_m (F) is gotten by the Langmuir isothermal adsorption model, G is [F/(a–b)].

Table 4. Kinetic adsorption model of adsorption of Pb^{2+}, Cu^{2+}, and Cd^{2+}

Adsorbent	Metal ion	First-order kinetic model				Second-order kinetic model		
		$q_{m,exp}$ / $(mg \cdot g^{-1})$	$q_{m,cal}$ / $(mg \cdot g^{-1})$	k_1 / $10^{-3} min^{-1}$	R^2	$q_{m,cal}$ / $(mg \cdot g^{-1})$	k_2 / $(10^{-4} L \cdot mg^{-1} \cdot min^{-1})$	R^2
α-Al_2O_3	Pb^{2+}	7.37	5.27	11.1	0.977	7.59	63.1	0.994
	Cu^{2+}	6.43	4.57	10.1	0.940	6.49	78.5	0.993
	Cd^{2+}	2.48	2.31	7.83	0.966	2.50	124	0.985
PAC[1]	Pb^{2+}	11.09	9.91	11.7	0.871	11.36	35.1	0.989
	Cu^{2+}	7.25	4.12	10.8	0.932	7.35	101	0.997
	Cd^{2+}	4.48	3.90	8.98	0.976	4.67	54.9	0.979
CNT[2]	Pb^{2+}	7.20	5.08	15.2	0.945	8.09	22.6	0.951
	Cu^{2+}	6.41	4.17	11.1	0.953	6.93	31.1	0.972
	Cd^{2+}	4.28	2.17	11.5	0.963	4.53	62.3	0.983
CNT/Al_2O_3	Pb^{2+}	40.23	29.17	19.1	0.897	47.17	2.99	0.930
	Cu^{2+}	24.96	17.14	15.2	0.946	28.17	6.54	0.956
	Cd^{2+}	11.18	9.50	12.9	0.845	11.85	44.3	0.991

Note: 1 represents active carbon powders, 2 represents commercial CNTs.

The amount of heavy metal adsorbed by adsorbent is greatly affected by the pH value of solution. Figs. 7(a)-(c) show the effect of pH value of solution on the amounts of Pb^{2+}, Cu^{2+}, and Cd^{2+} adsorbed by $CNTs/Al_2O_3$, commercial CNTs, active carbon powders, and Al_2O_3 particles respectively. In Fig. 7, the ordinate is the removal ratio (%) which is defined as the ratio of difference in concentration before and after adsorption to the concentration before adsorption. The removal ratio (%) is in general increased with an increase in pH value for all adsorbates and adsorbents. The pH value is 6.6 for $CNTs/Al_2O_3$, 6.8 for commercial CNTs, 7.6 for active carbon powders, and 8.2 for Al_2O_3 as 50% of Cd^{2+} is removed. The pH value is 6.4, 6.3, 6.7, and 8.1 for $CNTs/Al_2O_3$, commercial CNTs, active carbon powders, and Al_2O_3 particles respectively as 50% of Pb^{2+} is removed. It is worthy to note that $Cd(OH)_2$, $Cu(OH)_2$, and $Pb(OH)_2$ begin to precipitate at pH of 9, 9.4, and 9, respectively.

Figs. 8(a)-(c) show the removal ratio of Pb^{2+}, Cu^{2+}, and Cd^{2+} by various amounts of adsorbents, respectively. The removal ratio for all the adsorbates and adsorbents is in general increased with an increase in the amount of adsorbent. Among the removal ratio of Cd^{2+} by various adsorbents from 0.05 to 0.3 g, $CNTs/Al_2O_3$ is the largest, Al_2O_3 is the smallest, commercial CNTs and active carbon powders are almost at a same level. For the removal ratio of Pb^{2+} and Cu^{2+} by various ad-

sorbents, the order is $CNTs/Al_2O_3$>commercial CNTs>active carbon powders>Al_2O_3 particles except 0.05g of adsorbent at which active carbon powders>commercial CNTs for the removal of Cu. When the amount of $CNTs/Al_2O_3$ exceeds 0.2 g, the removal ratio of Cu^{2+} and Pb^{2+} is over 80%. When 0.3 g of $CNTs/Al_2O_3$ is used, the removal ratio of Cu^{2+} and Pb^{2+} almost reaches 100%.

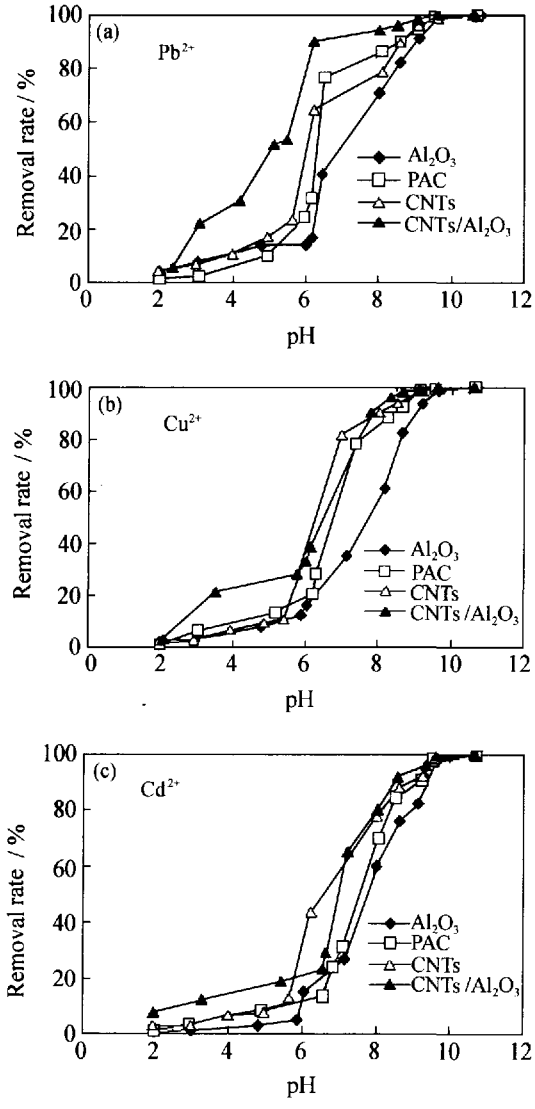

Fig. 7. Removal ratio of Cd^{+2} (a), Cu^{+2} (b), and Pb^{+2} (c) by various absorbents in various solutions with different pH values.

4. Conclusions

The as-grown $CNTs/Al_2O_3$ developed in this study has demonstrated an extraordinary absorption capacity without further treatment or oxidation [20] as well as dispersion property in water solution that the other CNTs lack.

The adsorption capacity of $CNTs/Al_2O_3$ for Pb^{2+}, Cu^{2+}, and Cd^{2+} from solutions is superior to that of active carbon powders, commercial CNTs, and Al_2O_3 particles. And, the order of amount adsorbed by $CNTs/Al_2O_3$ is Pb^{2+}>Cu^{2+}>Cd^{2+}. And the removal ratio of Pb^{2+}, Cu^{2+}, and Cd^{2+} adsorbed by $CNTs/Al_2O_3$ is increased with an increase in the amount of $CNTs/Al_2O_3$. The $CNTs/Al_2O_3$ has demonstrated a superior adsorption ability compared to other absorbents. In addition, the adsorption of Pb^{2+}, Cu^{2+}, and Cd^{2+} has occupied only a small surface area of $CNTs/Al_2O_3$.

For the isothermal adsorption behavior, the Langmuir isotherm is the best model for the adsorption of Pb^{2+}, Cu^{2+}, and Cd^{2+} by $CNTs/Al_2O_3$, commercial CNTs, active carbon powders, and Al_2O_3 particles. The calculated saturation amounts adsorbed by 1 g of $CNTs/Al_2O_3$ are 67.11, 26.59, and 8.89 mg/g for Pb^{2+}, Cu^{2+}, and Cd^{2+} respectively. For the kinetic behavior of the adsorption of Pb^{2+}, Cu^{2+}, and Cd^{2+} by $CNTs/Al_2O_3$, the second order kinetic model is the best one.

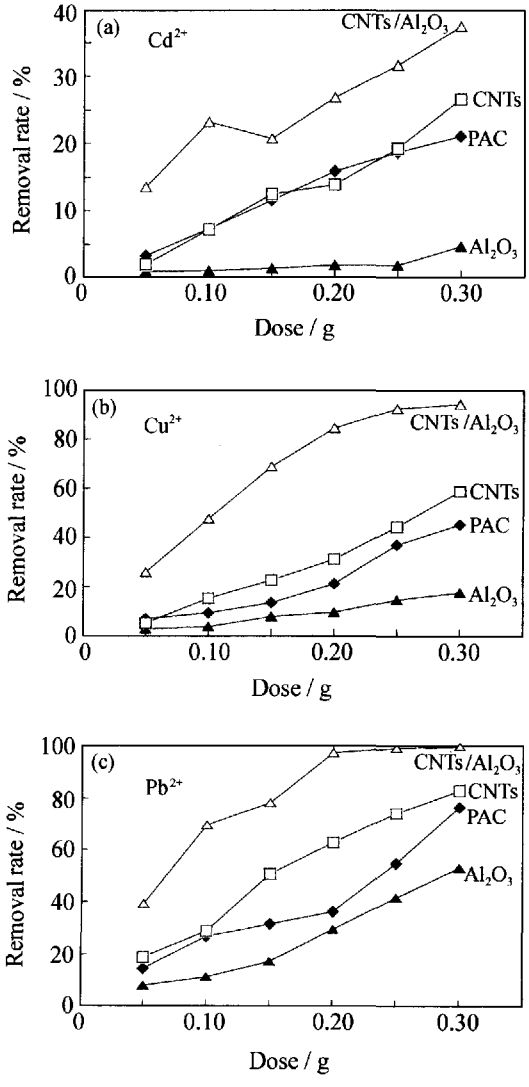

Fig. 8. Removal ratio of (a) Cd^{2+}, (b) Cu^{2+}, and (c) Pb^{2+} by various absorbents with different amounts.

Further researches on the usefulness of these composite nanoparticles in the future on practical applications are currently underway. It is also found that the adsorbed metal ions in the composite nanoparticles can be desorbed by concentrated HNO_3 and HCl. Thus, the regeneration of $CNTs/Al_2O_3$ can be promoted by in-

creasing the concentration of the acid. The recovery capacity is still maintained above 90% even after six successive adsorption-desorption cycles with Pb^{2+}/0.5 mol/L HNO_3 [21].

References

[1] Y.H. Li, J. Ding, Z. Luan, *et al.*, Competitive adsorption of Pb^{2+}, Cu^{2+}, Cd^{2+} ions from aqueous solutions by multiwalled carbon nanotubes, *Carbon*, 41(2003), p.2787.

[2] P.P. Julius and P.W. Linder, The adsorption characteristics of δ-manganese dioxide: A collection of diffuse double layer constants for the adsorption of H^+, Cu^{2+}, Ni^{2+}, Zn^{2+}, Cd^{2+} and Pb^{2+}, *Appl. Geochem.*, 16(2001), p.1067.

[3] S.A. Dastgheib and D.A. Rockstraw, A model for the adsorption of single metal ion solutes in aqueous solution onto activated carbon produced from pecan shells, *Carbon*, 40(2002), p.1843.

[4] M.F. Brigatti, C. Lugli, and L. Poppi, Kinetics of heavy-metal removal and recovery in sepiolite, *Appl. Clay Sci.*, 16(2000), p.45.

[5] Y. Yang and J. Shao, Synthesis of sulfhydryl chitin and its adsorption properties for heavy metals ions, *J. Appl. Polym. Sci.*, 77(2000), p.151.

[6] Z. Reddar, C. Gerente, Y. Andres, *et al.*, Adsorption of several metal ions onto a low-cost biosorbent: Kinetic and equilibrium studies, *Environ. Sci. Technol.*, 36(2002), p.2067.

[7] T. Jong and D.L. Parry, Adsorption of Pb(II), Cu(II), Cd(II), Zn(II), Ni(II), Fe(II) and As(V) on bacterially produced metal sulfides, *J. Colloid Interface Sci.*, 275(2004), p.61.

[8] A. Demirbas, E. Pehlivan, F. Gode, *et al.*, Adsorption of Cu(II), Zn(II), Ni(II), Pb(II), and Cd(II) from aqueous solution on amberlite IR-120 synthetic resin, *J. Colloid Interface Sci.*, 282(2005), p.20.

[9] S. Iijima, Helical microtubules of graphitic carbon, *Nature*, Vol. 354(1991), p.56.

[10] A.G. Rinzler, J.H. Hafner, P. Nikolaev, *et al.*, Unraveling nanotubes: field emission from an atomic wire, *Science*, 269(1995), 1550.

[11] G. Che, B.B. Lakshmi, E.R. Fisher, *et al.*, Carbon nanotubule membranes for electrochemical energy storage and production, *Nature*, 393(1998), p.346.

[12] B. Gao, A. Kelinhammes, X.P. Tang, *et al.*, Electrochemical intercalation of single-walled carbon nanotubes with lithium, *Chem. Phys. Lett.*, 307(1999), p.153.

[13] A. Bachtold, P. Hadley, T. Nakanishi, *et al.*, Logic circuits with carbon nanotube transistors, *Science*, 294(2001), p.1317.

[14] P.G. Collins and P. Avours, Nanotubes for electronics, *Sci. Am.*, 283(2000), p.62.

[15] R.Q. Long and R.T. Yang, Carbon nanotubes as superior sorbent for dioxin removal, *J. Am. Chem. Soc.*, 123(2001), p.2058.

[16] Y.H. Li, S. Wang, X. Zhang, *et al.*, Adsorption of fluoride from water by aligned carbon nanotubes, *Mater. Res. Bull.*, 38(2003), p.469.

[17] X. Peng, Y. Li, Z. Luan, *et al.*, Adsorption of 1,2-dichlorobenzene from water to carbon nanotubes, *Chem. Phys. Lett.*, 376(2003), p.154.

[18] Y.H. Li, S. Wang, J. Wei, *et al.*, Lead adsorption on carbon nanotubes, *Chem. Phys. Lett.*, 357(2002), p.263.

[19] Y.H. Li, S. Wang, and Z. Luan, Adsorption of cadmium (II) from aqueous solution by surface oxidized carbon nanotubes, *Carbon*, 41(2003), p.1057.

[20] S.H. Hsieh, J.J. Horng, and C.K. Tsai, Growth of carbon nanotube on micro-sized Al_2O_3 particle and its application to adsorption of metal ions, *J. Mater. Res.*, 21(2006), p. 1269.

[21] J.J. Horng, S.H. Hsieh, and C.K. Tsai, Metal adsorption of innovative composite carbon nanotubes in aqueous solution, *the 231st ACS National Meeting*, Atlanta, 2006, p. ENVR 94.